

# Surface Characteristics of Electrochemically Oxidized Implants and Acid-Etched Implants: Surface Chemistry, Morphology, Pore Configurations, Oxide Thickness, Crystal Structure, and Roughness

Young-Taeg Sul, DDS, PhD<sup>1</sup>/Eungsun Byon, PhD<sup>2</sup>/Ann Wennerberg, DDS, PhD<sup>3</sup>

**Purpose:** This study was undertaken to investigate surface properties of surface-modified titanium implants in terms of surface chemistry, morphology, pore characteristics, oxide thickness, crystal structure, and roughness. **Materials and Methods:** An oxidized, custom-made Mg implant, an oxidized commercially available implant (TiUnite), and a dual acid-etched surface (Osseotite) were investigated. Surface characteristics were evaluated with various surface analytic techniques. **Results:** Surface chemistry showed similar fingerprints of titanium oxide and carbon contaminant in common for all implants but also revealed essential differences of the elements such as about 9 at% Mg for the Mg implant, about 11 at% P for the TiUnite implant and about 12 at% Na for the Osseotite implant. Surface morphology of the Mg and TiUnite implants demonstrated a duplex oxide structure, ie, an inner barrier layer without pores and an outer porous layer with numerous pores, whereas the Osseotite implant revealed a crystallographically etched appearance with pits. The diameter and depth of pores/pits was  $\leq 2 \mu\text{m}$  and  $\leq 1.5 \mu\text{m}$  in the Mg implant,  $\leq 4 \mu\text{m}$  and  $\leq 10 \mu\text{m}$  in the TiUnite implant, and  $\leq 2 \mu\text{m}$  and  $\leq 1 \mu\text{m}$  in the Osseotite implant, respectively. Oxide layer revealed homogeneous thickness, about  $3.4 \mu\text{m}$  of all threads in the Mg implants. On the contrary, TiUnite showed heterogeneous oxide thickness, about 1 to  $11 \mu\text{m}$ , which gradually increased with thread numbers. Crystal structure showed a mixture of anatase and rutile phase for the Mg implants. With respect to roughness, Sa showed  $0.69 \mu\text{m}$  in the Mg implant,  $1.35 \mu\text{m}$  in the TiUnite implant, and  $0.72 \mu\text{m}$  in the Osseotite implant. **Conclusions:** Well-defined surface characterization may provide a scientific basis for a better understanding of the effects of the implant surface on the biological response. The surface-engineered implants resulted in various surface characteristics, as a result of different manufacturing techniques. INT J ORAL MAXILLOFAC IMPLANTS 2008;23:631–640

**Key words:** acid-etched surface, characterization of surface properties, oxidized Mg-incorporated surface, titanium implant

Surface innovation technology of titanium implants has been rapidly developing over the last 25 years so that now a wide variety of surface properties is applicable for different implant

systems.<sup>1–5</sup> The emerging trend of surface modification of clinical implants involves attempts at controlling surface chemistry,<sup>6–8</sup> and there is increasing demand for more sophisticated methods of characterization of implant surfaces. Detailed surface characterization is needed not only to advance our understanding of interfacial phenomena between the implant surface and tissues but also to aid the development of the next generation of implants.

A number of studies have reported that the surface properties of the implant direct the bone tissue responses<sup>9</sup> and eventually may play a critical role in their clinical success.<sup>10</sup> However, despite the great importance of surface properties, there is no consensus about the extent to which surface properties are correlated with bone response and about what standards should be used for surface analyses. Surface roughness is the parameter that has been most

<sup>1</sup>Associate Professor, Department of Biomaterials/Handicap Research, Institute for Clinical Sciences, Sahlgrenska Academy at Göteborg University, Göteborg, Sweden.

<sup>2</sup>Senior Researcher, Department of Surface Engineering, Korea Institute of Machinery and Materials, Changwon, Korea.

<sup>3</sup>Professor, Department of Biomaterials/Handicap Research, Department of Prosthetic Dentistry/Dental Material Science, Göteborg University, Göteborg, Sweden.

**Correspondence to:** Dr Young-Taeg Sul, Department of Biomaterials/Handicap Research, Institute for Clinical Sciences, Göteborg University, Box 412, S-405 30, Göteborg, Sweden. Fax: +46 31 773 2941. E-mail: young-taeg.sul@biomaterials.gu.se

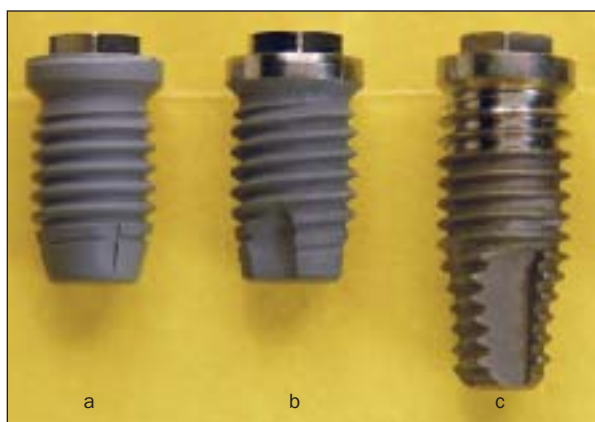


**Fig 1** The 3 implant types used in the study: (a) the magnesium implant, (b) the TiUnite implant, and (c) the Osseotite implant.

widely investigated.<sup>11,12</sup> Studies of surface roughness have indicated that moderately rough surfaces seem to show advantageous outcomes. Previous studies from the authors' laboratory documented that *in vivo* bone response can be significantly enhanced by improving surface oxide properties of implants such as surface chemistry, surface roughness, oxide thickness, and morphology (pore characteristics and crystal structures).<sup>9,13–15</sup> Surface chemistry seems certainly to be a key factor for improvement of osseointegration.<sup>9,15–17</sup>

The present study follows up on a recent publication on the effects of surface properties of an oxidized magnesium implant, TiUnite, and Osseotite on the bone response.<sup>17</sup> Sul et al have reported significant differences of rate and strength of osseointegration and osteoconductivity when comparing these to one another. The aim of the present study was to characterize in greater detail surface properties of the oxidized magnesium, TiUnite, and Osseotite implants and, furthermore, to analyze the validity of the previous conclusion<sup>17</sup>: that of the surface properties investigated, surface chemistry was the most determinant parameter and facilitated more rapid and stronger osseointegration of the magnesium implant despite its minimal roughness as compared to the TiUnite and Osseotite surfaces.

## MATERIALS AND METHODS

Three groups of screw-shaped titanium implants (Fig 1), one custom-made magnesium implant of 3.75 mm in diameter and 7 mm length and 2 commercially available clinical implants, an oxidized TiUnite design (3.75 × 7 mm, Nobel Biocare, Göteborg, Swe-

den) and a dual acid-etched Osseotite (3.75 × 8.5 mm, Biomet/3i, Palm Beach Gardens, FL), were investigated. The magnesium implant was prepared in a mixed electrolyte containing magnesium ions using the microarc oxidation (MAO) method in galvanostatic mode. The MAO method used in the present study has been described in previous studies.<sup>2,20</sup> In brief, the electrochemical cell was composed of 2 platinum plates as cathodes, with a titanium anode at the center. The platinum cathodes had surface areas of 16 cm<sup>2</sup>. Currents and voltages were continuously recorded at intervals of 1 second by an IBM computer interfaced with a DC power supply. The content of ripple was controlled to less than 0.1%. During the MAO process, the anodic-forming voltage (with slope  $dV/dt$ ) was controlled at  $\geq 0.5$  V/sec with combined electrochemical parameters. The clinical implants were purchased from local distributors. In the case of the Osseotite implant, this study evaluated its acid-etched surface but not the polished area of the upper threads of the same implant.

Surface chemistry was analyzed by x-ray photoelectron spectroscopy (XPS, ESCALAB 250; VG Scientific, West Sussex, England). The XPS spectra were recorded using normal Al K $\alpha$  radiation (1486.6 eV) with a probing beam size of 200  $\mu$ m. All samples were measured twice, ie, once as received and then after argon (Ar<sup>2+</sup>) sputter cleaning. To evaluate after cleaning, ie, removal of surface contaminants, the as-received surfaces were prepared by etching with argon ions of an ion energy of 5 keV and a beam current of 0.3  $\mu$ A for 150 seconds. The removed outermost surface layer was estimated as about 2 nm in thickness. The binding energies of the photoelectron peaks were referenced to the C (1s) line at 284.5 eV.

Surface morphology was characterized by scanning electron microscopy (SEM, JSM-6700F; JEOL, Tokyo, Japan). All the samples were coated with a thin layer of gold to reduce the electric charge that builds up rapidly in specimens scanned by a beam of high-energy electrons.

The oxide thickness and pore configurations of the oxidized implants were measured with focal emission mode (FE-SEM) on cross sections prepared by the metallurgical method of nickel plating.<sup>18</sup>

The crystal structure of the magnesium implant was determined by using low-angle x-ray diffraction with a thin film collimator (X'Pert PRO-MRD; Philips, Washington DC) on a plate-type sample prepared with the same electrochemical parameters as the test screw-shaped implants. The step size was 0.02 degrees between 15 and 70 degrees of measured scans. Spectra were recorded using Cu K $\alpha$  radiation (0.154056 Å) generated at an acceleration voltage of 35 kV and a current of 25 mA.

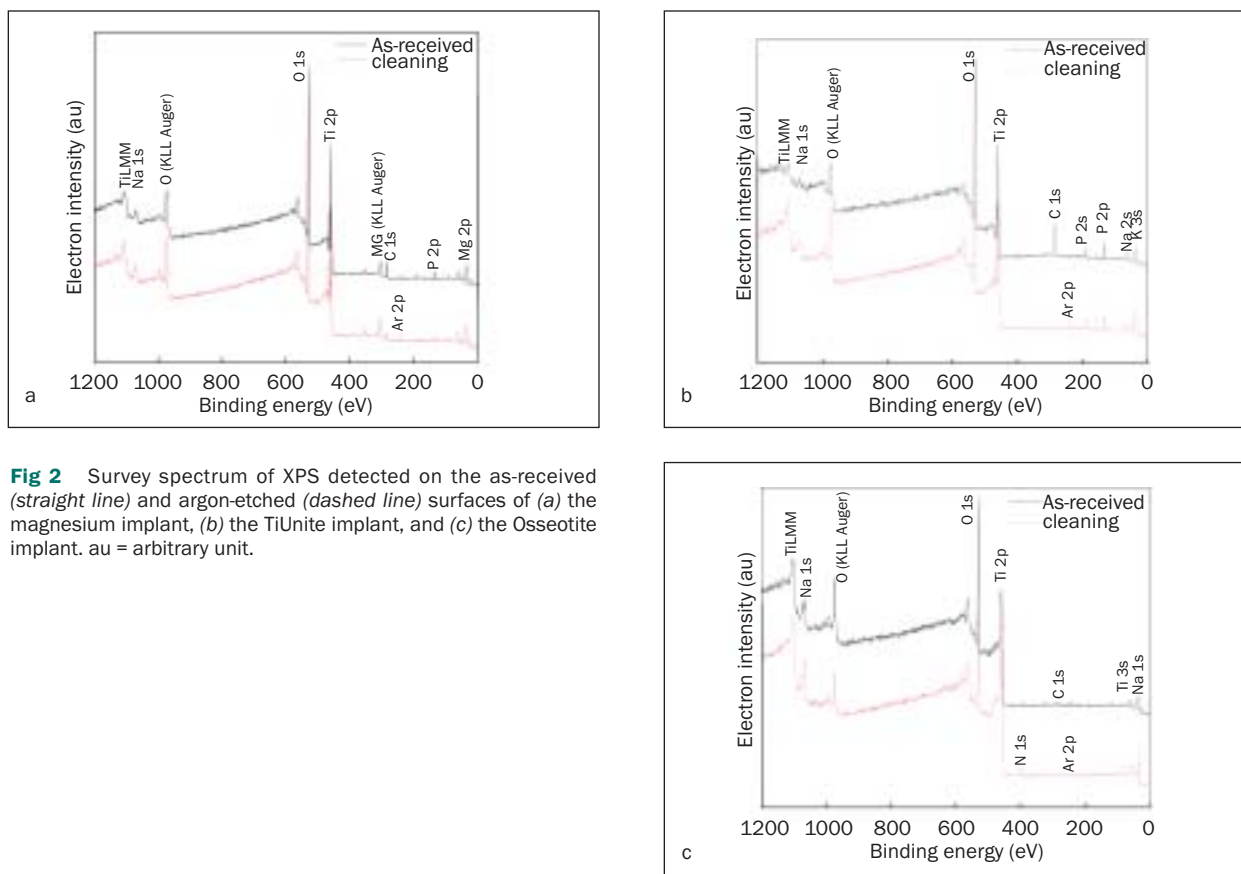


**Fig 2** Survey spectrum of XPS detected on the as-received (straight line) and argon-etched (dashed line) surfaces of (a) the magnesium implant, (b) the TiUnite implant, and (c) the Osseotite implant. au = arbitrary unit.

Surface roughness was measured with Optical Interferometry (MicroXam<sup>TM</sup>; Phase-Shift, Tucson, AZ). Two screws from each manufacture were selected and measured on 3 thread tops, 3 thread valleys, and 3 thread flanks each, making 18 measurements for each group. The measuring area was  $260 \mu\text{m} \times 200 \mu\text{m}$  for each measurement. A Gaussian filter was used to separate roughness from error of form and waviness. The filter size was set to  $50 \mu\text{m} \times 50 \mu\text{m}$ .

## RESULTS

Figure 2 demonstrates the XPS survey spectra of the implants. All spectra revealed common chemicals of titanium oxides, ie, titanium, oxygen, and carbon (a contaminant). Figure 3a shows a doublet peak of Ti 2p spectrum at  $\approx 458.5 \text{ eV}$  and  $464.3 \text{ eV}$  for all implants. In addition, a broad shoulder at  $\approx 453.5 \text{ eV}$  was detected in the high-resolution spectrum for Osseotite implants. The high resolution spectra of O 1s and C 1s in Figs 3b and 3c demonstrates similar peaks at  $\approx 530 \text{ eV}$  and at  $\approx 284.5 \text{ eV}$  for all surfaces. The spectra of O and C revealed broadenings (rela-

tively higher intensity peaks) at 532 to 533 eV for the magnesium implants and at 288.2 eV for TiUnite and Osseotite, respectively. Figure 4 presents high-resolution spectra of the most distinguishable surface elements between the implants, ie, Mg 2p at  $\approx 50.05 \text{ eV}$  for the magnesium implants, P 2p<sub>3/2</sub> at  $\approx 130.7 \text{ eV}$  for TiUnite, and Na 1s at  $\approx 1072 \text{ eV}$  for Osseotite. The quantitative analyses of surface elements are shown in Table 1.

Figures 5 to 7 show overall SEM morphologies of the implants. The thread geometry of the magnesium implant showed a more rounded thread design as compared to TiUnite and Osseotite. The oxidized magnesium implants and TiUnite implants revealed a duplex oxide structure consisting of an outer porous layer with numerous pores and an inner barrier layer without pores (Figs 5 to 8). Figure 8 presents cross-sectional views of the surface oxide. TiUnite showed a barrier film structure with sparse pores at the first and second threads and a porous film structure with more pores toward the apical end of the implant, eg, the fourth and fifth threads (Figs 8b to 8d). In contrast, the magnesium and Osseotite implants showed a homogeneous film structure in all threads (Figs 8a and 8e). There were differences of

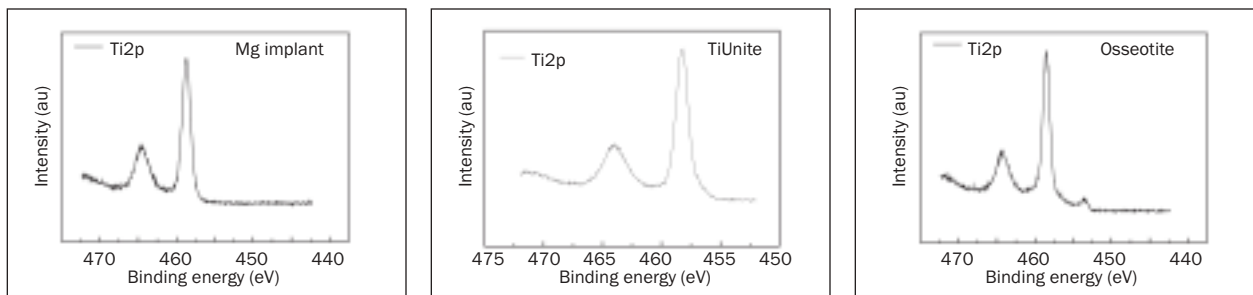


**Fig 3a** Comparisons of Ti 2p spectra at XPS high resolution between the magnesium, TiUnite, and Osseotite implants.

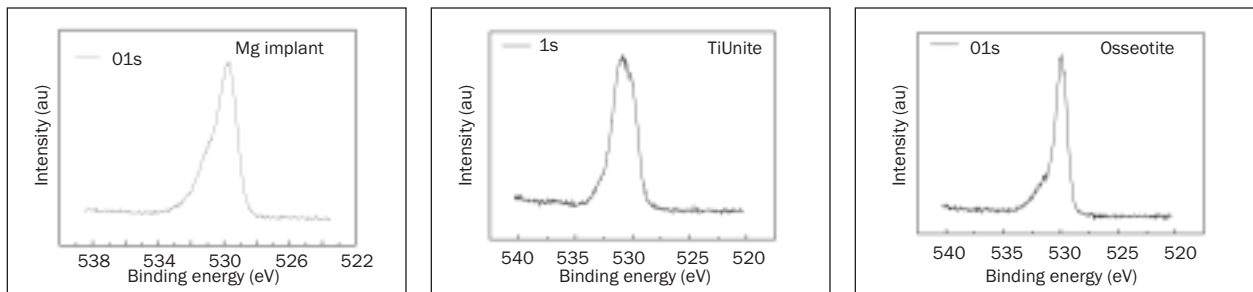


**Fig 3b** Comparisons of O 1s spectra at XPS high resolution between the magnesium, TiUnite, and Osseotite implants.

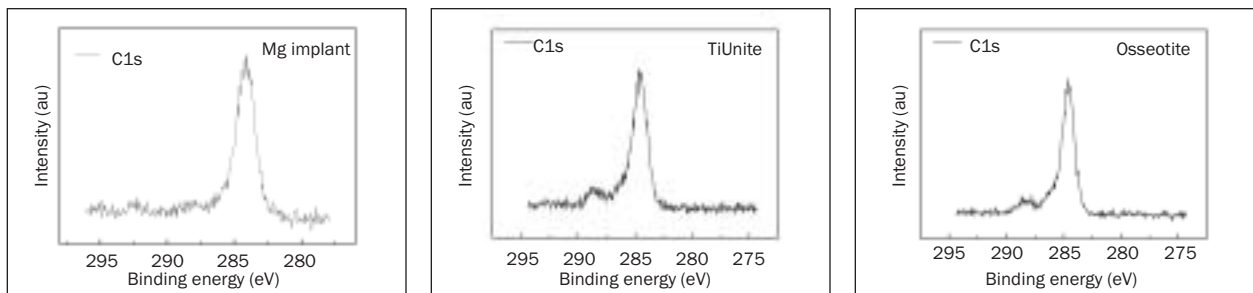


**Fig 3c** Comparisons of C 1s spectra at XPS high resolution between the magnesium, TiUnite, and Osseotite implants.

**Fig 4a** XPS high-resolution spectra of the representative element detected on the as-received and Ar-etched surfaces, Mg (Mg 2p) in the magnesium implant surface.

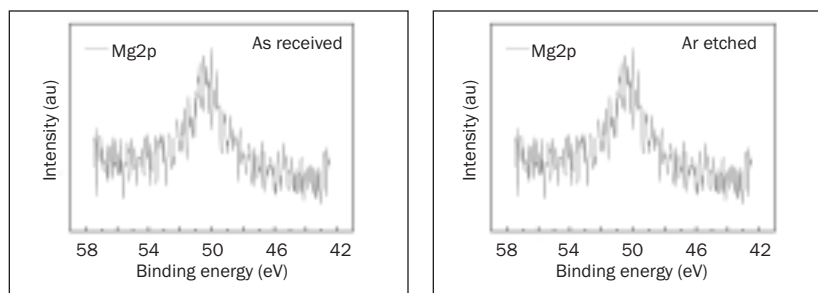


**Fig 4b** XPS high-resolution spectra of the representative element detected on the as-received and Ar-etched surfaces, P (P 2p) in the TiUnite implant surface.

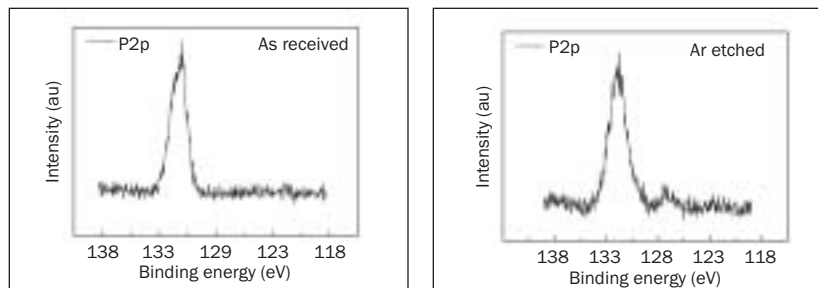


**Fig 4c** XPS high-resolution spectra of the representative element detected on the as-received and Ar-etched surfaces, Na (Na 1s) in the Osseotite implant surface.

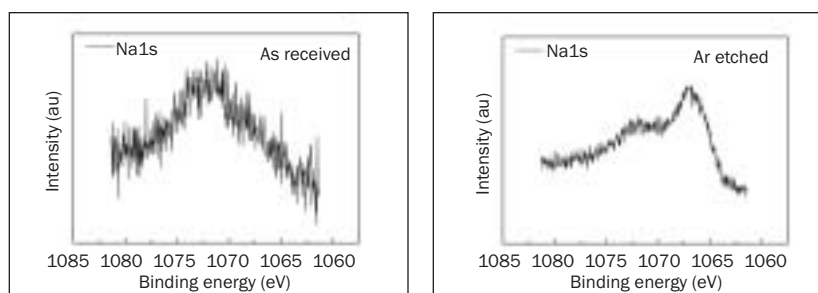


**Table 1** Quantitative Analyses of the Surface Elements at Relative Atom Concentrations (at%)

Element composition	Mg implant		TiUnite		Osseotite	
	As-received*	After cleaning <sup>†</sup>	As-received*	After cleaning <sup>†</sup>	As-received*	After cleaning <sup>†</sup>
Ti 2p	18.8	21.1	13.0	22.0	15.6	36.7
O 1s	53.4	57.3	50.5	56.4	48.4	40.7
C 1s	15.2	3.0	24.3	2.1	34.2	3.7
Mg 2p	7.6	9.3	-	-	-	-
P 2p	2.3	2.7	9.7	10.9	-	-
Na 1s	1	3	0.5	3.8	0.7	11.8
N 1s	0.5	0.5	0.6	1.5	1.0	4.8
S 1s	1.0	0.8	1.2	1	trace	trace
Ar		2.0		2.1		2.1

\*As detected when the implants were received.

<sup>†</sup>After 150 seconds of Ar<sup>+</sup> sputter cleaning.

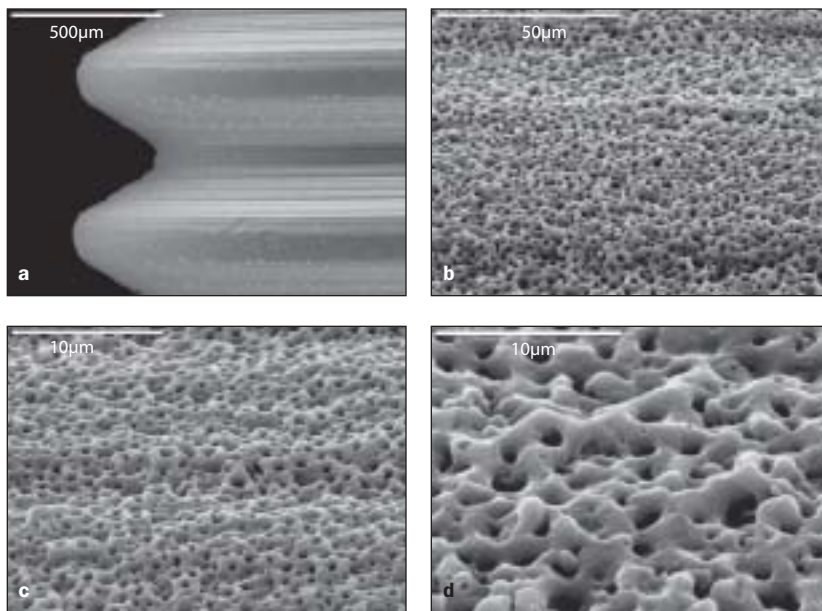


**Fig 5** SEM images of the magnesium implant at resolutions of (a) 150 $\times$ , (b) 1,000 $\times$ , (c) 5,000 $\times$ , and (d) 10,000 $\times$ .

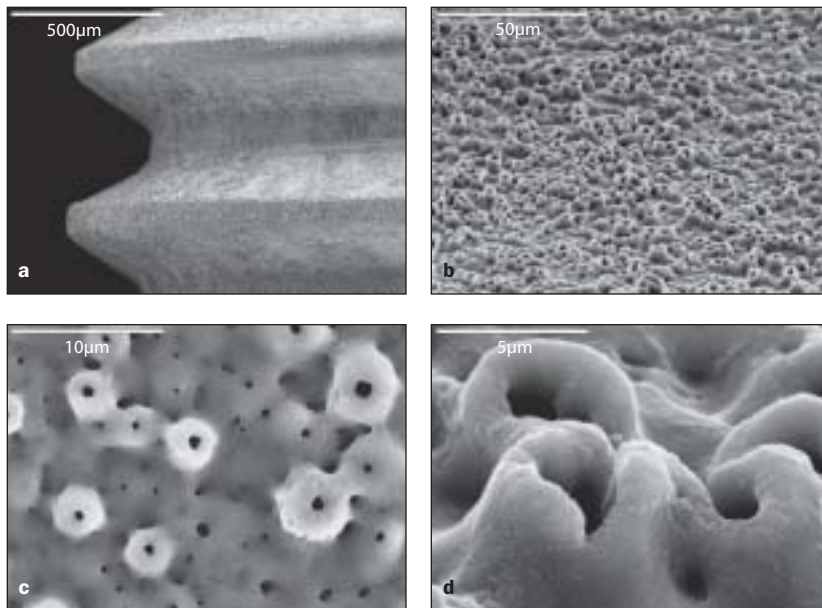


**Fig 6** SEM images of TiUnite implant at the different resolutions of (a) 150 $\times$ , (b) 1,000 $\times$ , (c) 5,000 $\times$ , and (d) 10,000 $\times$ .

“open pore” structures between the magnesium implant and TiUnite. Pores in the magnesium implants had a less elevated margin than those in TiUnite implants. The pore/pit size (diameter) was  $\leq 2 \mu\text{m}$  in the magnesium and Osseotite implants but  $\leq 4 \mu\text{m}$  in the TiUnite implants. The pore/pit depth was  $\leq 1.5 \mu\text{m}$  in the magnesium implant,  $\leq 10 \mu\text{m}$  in the TiUnite implant, and  $\leq 1 \mu\text{m}$  in the Osseotite implant.

Pore population in the magnesium implants was denser than in the TiUnite implants. Crack propagation was sometimes observed in the surface oxide of TiUnite (Fig 6c).

The oxide thicknesses measured in the cross sections of the surface oxide (Fig 8) revealed about a thickness of about  $3.4 \mu\text{m}$  for the magnesium implant ( $n = 15$ ,  $SD = 0.6$ ), about  $4 \mu\text{m}$  at the first

**Fig 7** SEM images of Osseotite implant at the different resolutions of (a) 150 $\times$ , (b) 1000 $\times$ , (c) 5000 $\times$ , and (d) 10,000 $\times$ .

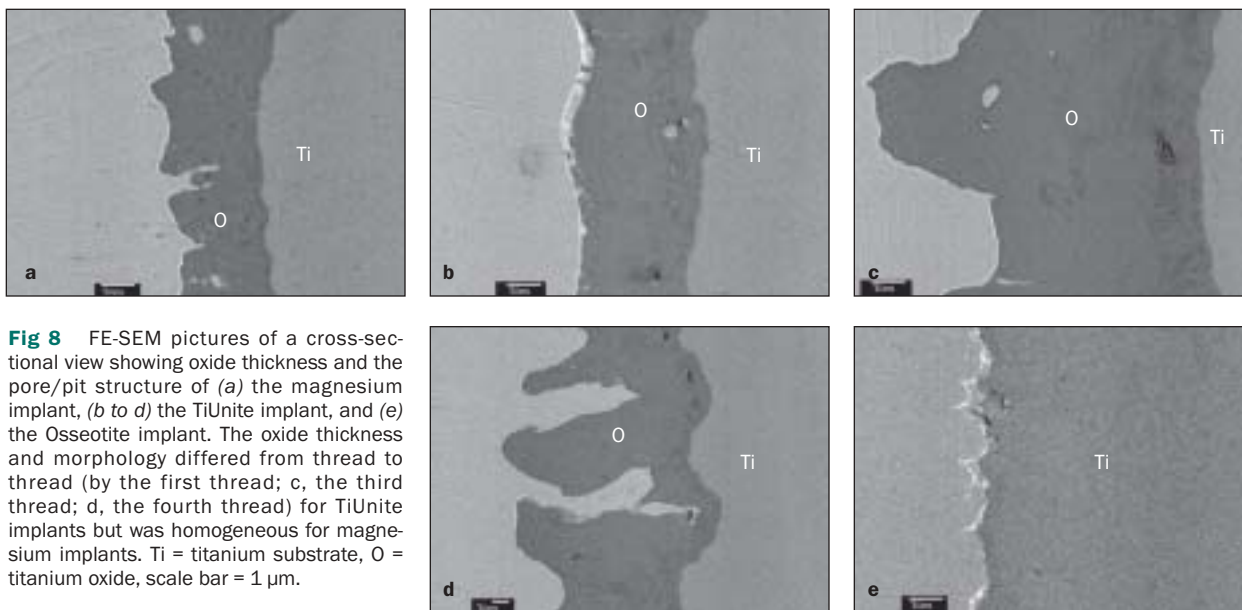
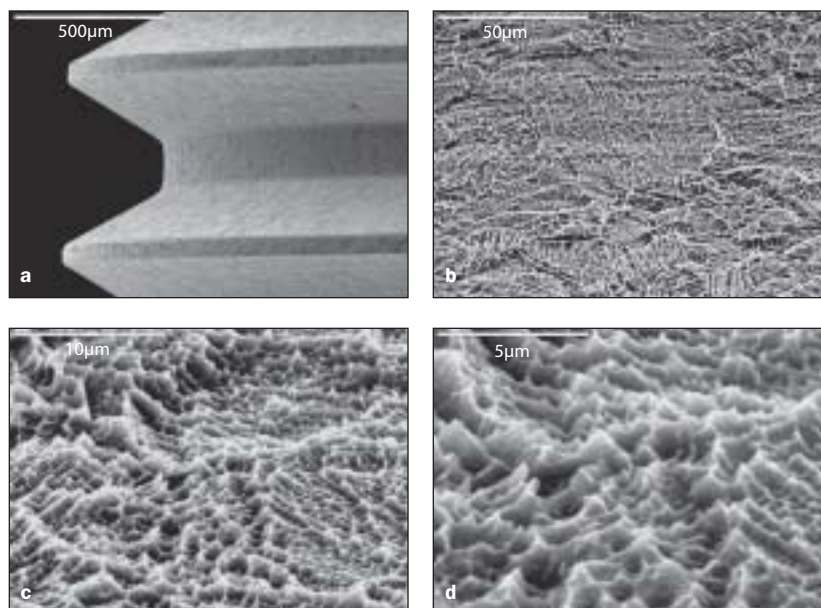


**Fig 8** FE-SEM pictures of a cross-sectional view showing oxide thickness and the pore/pit structure of (a) the magnesium implant, (b to d) the TiUnite implant, and (e) the Osseotite implant. The oxide thickness and morphology differed from thread to thread (by the first thread; c, the third thread; d, the fourth thread) for TiUnite implants but was homogeneous for magnesium implants. Ti = titanium substrate, O = titanium oxide, scale bar = 1  $\mu$ m.

thread, about 1 to 9  $\mu$ m at the third thread, about 1 to 6  $\mu$ m at the bottom (barrier film), and about 11  $\mu$ m at the pore top (porous film) of the fifth thread. The oxide thickness of Osseotite was too thin to measure by FE-SEM. Crystal structure of the surface oxide by XRD measurements showed a mixture of anatase and rutile for both the magnesium (Fig 9) and TiUnite implants.<sup>6</sup>

The surface roughness corresponding to the magnesium, TiUnite, and Osseotite implants was measured in terms of arithmetic average height deviation ( $S_a$ ); developed surface ratio, ie, the ratio of the increment of the interfacial area of a surface over the sampling area ( $S_{dr}$ ); and the number of summits of a unit sampling area ( $S_{ds}$ ). The surface characteristics of the implants are summarized in Table 2.

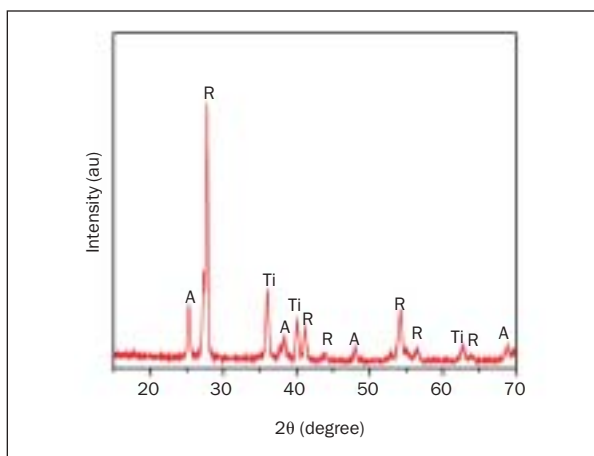


**Fig 9** XRD diffraction pattern on commercially pure titanium plates abraded by 800-grit SiC paper and oxidized in the same manner as the magnesium implant (acceleration voltage of 35 kV and current of 25 mA). A refers to the anatase phase and R to the rutile phase.

**Table 2** Summary of Surface Characteristics of the Implants

Surface Property	Mg implant	TiUnite	Osseotite
Chemical composition	Mainly TiO <sub>2</sub> , Mg ≤ 9.3 at%, P ≤ 3 at%. Contaminant: C ≤ 15 at%. Traces: S	Mainly TiO <sub>2</sub> , ≤ 10.9 at%. Contaminant: C ≤ 24 at%, Na ≤ 4 at%, N ≤ 1.5 at%. Traces: S	Mainly TiO <sub>2</sub> . Contaminant: C ≤ 34 at%, Na ≤ 18 at%, N ≤ 4.8%. Traces: S
Morphology	Duplex oxide structure The outer porous film with micropores and the inner barrier film without micropores	Duplex oxide structure The outer porous film with micropores and the inner barrier film without micropores	Grain boundary orientation (× 1,000) Micropits-texture at high magnification (× 10,000)
Pore/pit size	≤ 2 μm	≤ 4 μm	≤ 2 μm
Oxide thickness			
Homogeneity	Homogenous	Heterogenous	
Porous film	3.4 μm at all the threads	5.7 μm at the 1st thread 5.9 μm at the 3rd thread 5.3 μm at the 5th thread	0.003 to 0.014 μm*
Barrier film	1.3 to 2 μm	0.9 to 5.0 μm	
Crystal structure	Anatase + rutile	Anatase + rutile**	Amorphous**
Roughness			
Sa (μm)	0.69 ± 0.24	1.35 ± 0.16	0.72 ± 0.42
Sdr (%)	26.4 ± 11.5	125.3 ± 37.3	28.6 ± 16.0
Sds (μm <sup>2</sup> )	0.12 ± 0.04	0.06 ± 0.01	0.12 ± 0.05

Chemical elements were measured at relative atomic concentration (at%) after Ar+ sputter cleaning of oxide 2 nm thick.

\*No determination possible. In general, however, the nave oxide thickness is known to be in the range of 3 to 14 nm.<sup>19</sup>

\*\*Crystal structure was not measurable on the screw-type implants of TiUnite and Osseotite as supplied by the manufacturers; this information was obtained from a reference.<sup>6</sup> A thin oxide layer in the range of 3 to 14 nm is known to be amorphous.<sup>20</sup>

Sa = arithmetic average height deviation; Sdr = developed surface ratio, ie, the ratio of the increment of the interfacial area of a surface over the sampling area (%); Sds = the number of summits of a unit sampling area.

## DISCUSSION

A previous study reported significantly more rapid and stronger bone response to the Mg implant compared to the TiUnite and Osseotite implants.<sup>17</sup> Removal torques were 27.1 Ncm for the magnesium implant, 21.3 for the TiUnite implant, and 15.4 for the Osseotite implant. At 3 weeks, new bone formation values of 29% for the magnesium implant, 18% for the TiUnite implant, and 15% for the Osseotite implant were registered, respectively. At 6 weeks, the removal torque values were 37.5 Ncm, 36.4 Ncm, and 21.5 Ncm, respec-

tively, whereas new bone formation was 39%, 31%, and 26%, respectively. The present study presents more detailed information on the surface properties of magnesium, TiUnite, and Osseotite implants in an effort to highlight the significant contribution of the surface properties to the bone response.

Of the surface properties examined, the greatest differences among the 3 implants were detected in surface chemistry (Table 1). This is due to the differences of the surface treatment used, ie, electrochemical oxidation for the magnesium and TiUnite implants and a dual-acid etching technique for the

Osseotite implant. The acid-etching and blasting methods generally do not change the main compositional surface elements of the titanium, which consist mainly of titanium and oxygen, but rather the surface morphology/topography and consequently surface roughness. In contrast, the electrochemical MAO process changes surface chemistry as well as the oxide thickness, surface morphology/topography, crystal structure, and surface roughness.<sup>20</sup> Those surface properties greatly depend on the electrochemical parameters of the MAO process used, particularly the preferred electrolyte. In general, porosity and crystallinity of the titanium oxide increase with increase of the breakdown voltage.<sup>2,20</sup>

As-received surfaces of all implants showed a similar range of percentage of titanium (13% to 19%) and oxygen (48% to 53%). Carbon content showed big differences among the implants: 15% in the Mg implant, 24% in the TiUnite implant, and 34% in the Osseotite implant. After sputter cleaning with argon ions (an ion energy of 5 keV and a beam current of 0.3  $\mu$ A for 150 seconds), corresponding to 2 nm in thickness, titanium and oxygen content of the magnesium and TiUnite implants increased to the same level of 22 at% and around 57%, respectively. In contrast, the Osseotite implants showed a decrease of oxygen content and an abrupt increase of titanium. The peak of the C 1s in all 3 implants was dominated at 285 eV (spectra not shown). After argon sputter cleaning, C disappeared (ie, dropped to the 2% to 4% level) for all the implants. This result indicates that the presence of carbon species is essentially not a constituent of the surface oxide layer but rather attributable to surface contamination given by absorbed organic carbon-containing molecules<sup>21</sup> to the outermost surface layer (2 nm). The Osseotite implant was most contaminated with carbon; the percentage of carbon dropped from 34% to 4% after sputter cleaning. In essence, the most distinguishable surface elements between the implants were magnesium for the magnesium implants, phosphorus for the TiUnite implants, and sodium 1s for the Osseotite implants. The magnesium and TiUnite implants showed obvious differences of surface chemistry by field-assisted migration of anions, although the oxide films occurred during the MAO process, such as some 9 at% magnesium for the magnesium implant and some 11 at% phosphorus in TiUnite. Apart from magnesium and TiUnite implants, the Osseotite implant showed a relatively high concentration of sodium of some 12 at%. The presence of some 1 at% sulfur in the magnesium and TiUnite implants may not indicate a trace but probably was incorporated from the electrolyte system employed.<sup>6,22</sup> Such systemic changes of surface chemistry strongly depend on the electrochemical

parameters of the system employed, such as concentration, composition, mixture rate, and pH.<sup>2,20</sup>

The surface morphologies and oxide structure of the magnesium and TiUnite implants showed some similarities and some differences, but the Osseotite implant substantially differed from the other two. The magnesium implant and TiUnite implant showed a double layer structure, ie, an outer porous layer with numerous pores and an inner barrier without pores. However, the oxide thickness of the magnesium implant, 3.4  $\mu$ m, is thinner and more homogeneous as compared to the TiUnite implant, showing a thickness of 1  $\mu$ m at the bottom of barrier film and about 11  $\mu$ m at the pore top of porous film. The oxide thickness of the Osseotite implant was known to be about 5.7 nm from the literature.<sup>19</sup> Some open pores were fused to one another and became larger and irregular in shape. Some pores, so-called closed pores, seemed to be interconnected to one another. The TiUnite implant showed the most elevated margin of pores. This may explain why the TiUnite implant showed the highest roughness values with respect to the height deviation and surface enlargement. One reason for the crack propagation on the surface oxide of TiUnite in Fig 6c may be the involvement of this "thicker" oxide layer with the employed electrochemical parameters. The surface morphology of the Osseotite implant can be characterized by "crystallographically etched appearance" at the coarse grain structure (see the orientation of individual grains in Figs 7b and 7c) and also featured with micropits of needle-like margin structure,  $\leq 2$   $\mu$ m wide and  $\leq 1$   $\mu$ m deep in the high resolution of cross-section view. Massaro et al in 2002 reported that when local dissolution rates depend on the orientation of the individual titanium grains, a crystallographically etched structure appeared.<sup>19</sup> Since there are limitations of XRD instrumentation on the screw-shaped implants, the crystal structure in the present study was measured on a plate-type sample prepared with the same electrochemical parameters as the test screw-shaped implants. Thus, there is a need for further verification of the crystal structures of the implants in the present study.

## CONCLUSIONS

Electrochemical oxidation and acid-etching of the implant surfaces developed different surface properties in terms of surface chemistry, morphology, pore characteristics, oxide thickness, crystal structure, and roughness. The MAO method resulted in obvious differences of surface chemistry with magnesium cations incorporated for the magnesium implant and phosphorus anions incorporated for the TiUnite implant.

## ACKNOWLEDGMENTS

This work was supported by the research grants of the development project (2007-04306) from the Ministry of Science and Technology, Republic of Korea, MediSciTec, the Sylvan Foundation, and the Swedish Research Council.

## REFERENCES

1. Bosetti M, Masse A, Tobin E, Cannas M. In vivo evaluation of bone tissue behavior on ion implanted surfaces. *J Mater Sci Mater Med* 2001;12:431–435.
2. Sul YT, Johansson CB, Jeong Y, Albrektsson T. The electrochemical oxide growth behaviour on titanium in acid and alkaline electrolytes. *Med Eng Phys* 2001;23:329–346.
3. Kasemo B. Biological surface science. *Surf Sci* 2002;500:656–677.
4. Kokubo T, Kim HM, Kawashita M, Nakamura T. Bioactive metals: Preparation and properties. *J Mater Sci Mater Med* 2004;15:99–107.
5. Nayab SN, Jones FH, Olsen I. Effects of calcium ion implantation on human bone cell interaction with titanium. *Biomaterials* 2005;26:4717–4727.
6. Hall J, Lausmaa J. Properties of a new porous oxide surface on titanium implants. *Appl Osseointegration Res* 2001;1:5–8.
7. Ellingsen JE, Johansson CB, Wennerberg A, Holmen A. Improved retention and bone-implant contact with fluoride-modified titanium implants. *Int J Oral Maxillofac Implants* 2004;19:659–666.
8. Buser D, Broggini N, Wieland M, et al. Enhanced bone apposition to a chemically modified SLA titanium surface. *J Dent Res* 2004;83:529–533.
9. Sul YT. The significance of the surface properties of oxidized titanium implant to the bone response: Special emphasis on potential biochemical bonding of oxidized titanium implants. *Biomaterials* 2003;24:3893–3907.
10. Albrektsson T, Wennerberg A. Oral implant surfaces: Part 1—review focusing on topographic and chemical properties of different surfaces and in vivo responses to them. *Int J Prosthodont* 2004;17:536–543.
11. Wong M, Eulenberger J, Schenk R, Hunziker E. Effect of surface topology on the osseointegration of implant materials in trabecular bone. *J Biomed Mater Res* 1995;29:1567–1575.
12. Wennerberg A, Ektessabi A, Albrektsson T, Johansson C, Andersson B. A 1-year follow-up of implants of differing surface roughness placed in rabbit bone. *Int J Oral Maxillofac Implants* 1997;12:486–494.
13. Sul YT, Johansson CB, Jeong Y, Röser K, Wennerberg A, Albrektsson T. Oxidized implants and their influence on the bone response. *J Mater Sci Mater Med* 2001;12:1025–1031.
14. Sul YT, Byon E, Jeong Y. Biomechanical measurements of calcium-incorporated, oxidized implants in rabbit bone: Effect of calcium surface chemistry of a novel implant. *Clin Implant Dent Relat Res* 2004;6:101–110.
15. Sul YT, Johansson CB, Wennerberg A, Cho LR, Chang BS, Albrektsson T. Optimizing surface oxide properties of oxidized implants for reinforcement of osseointegration: Surface chemistry, oxide thickness, porosity, roughness, crystal structure. *Int J Oral Maxillofac Implants* 2005;20:349–359.
16. Sul YT, Johansson CB, Byon E, Albrektsson T. The bone response of oxidized bioactive and non-bioactive titanium implants. *Biomaterials* 2005;26:6720–6730.
17. Sul YT, Johansson CB, Albrektsson T. Which surface properties enhance bone response to implants? Comparison of oxidized Mg implant, TiUnite and Osseotite surfaces. *Int J Prosthodont* 2006;19:319–328.
18. Nakao S, Kim DH, Obata K, et al. Electroless pure nickel plating process with continuous electrolytic regeneration system. *Surf Coat Technol* 2003;169:132–134.
19. Massaro C, Rotolo P, De Riccardis F, et al. Comparative investigation of the surface properties of commercial titanium dental implants. Part I: chemical composition. *J Mater Sci Mater Med* 2002;13:535–548.
20. Sul YT, Johansson CB, Petronis S, et al. Characteristics of the surface oxides on turned and electrochemically oxidized pure titanium implants up to dielectric breakdown: The oxide thickness, micropore configurations, surface roughness, crystal structure and chemical composition. *Biomaterials* 2002;23:491–501.
21. Lausmaa J, Kasemo B. Surface spectroscopic characterization of titanium implant materials. *Appl Surf Sci* 1990;44:133–146.
22. Sul YT, Johansson P, Chang BS, Byon E, Jeong Y. Bone response to Mg-incorporated, oxidized implants in rabbit femur: Mechanical interlocking vs Biochemical bonding. *J Appl Biomater Biomech* 2005; 3: 18–28.